

# Density of States in the Magnetic Ground State of the Friedel-Anderson Impurity

Gerd Bergmann  
Department of Physics  
University of Southern California  
Los Angeles, California 90089-0484  
e-mail: bergmann@usc.edu

August 23, 2021

## Abstract

By applying a magnetic field whose Zeeman energy exceeds the Kondo energy by an order of magnitude the ground state of the Friedel-Anderson impurity is a magnetic state. In recent years the author introduced the Friedel Artificially Inserted Resonance (FAIR) method to investigate impurity properties. Within this FAIR approach the magnetic ground state is derived. Its full excitation spectrum and the composition of the excitations is calculated and numerically evaluated. From the excitation spectrum the electron density of states is calculated. Majority and minority d-resonances are obtained. The width of the resonances is about twice as wide as the mean field theory predicts. This broadening is due to the fact that any change of the occupation of the d-state in one spin band changes the eigenstates in the opposite spin band and causes transitions in both spin bands. This broadening reduces the height of the resonance curve and therefore the density of states by a factor of two. This yields an intuitive understanding for a previous result of the FAIR approach that the critical value of the Coulomb interaction for the formation of a magnetic moment is twice as large as the mean field theory predicts.

PACS: 75.20.Hr, 71.23.An, 71.27.+a

# 1 Introduction

The properties of magnetic impurities in a metal is one of the most intensively studied problems in solid state physics. The work of Friedel [1] and Anderson [2] laid the foundation to understand why some transition-metal impurities form a local magnetic moment while others don't. Kondo [3] showed that multiple scattering of conduction electrons by a magnetic impurity yields a divergent contribution to the resistance in perturbation theory. Yoshida [4] introduced the concept that the (spin 1/2) magnetic impurity forms a singlet state with the conduction electrons and is non-magnetic at zero temperature. These new insights stimulated a large body of theoretical and experimental work (see for example [4], [5], [6], [7], [8], [9], [10], [11], [12], [13]).

The majority of experimental and theoretical work has focussed on the singlet Kondo ground state. However, the "magnetic state" of the impurity is of equal or even greater importance because magnetic impurities are always present, including in micro-chips and nanostructures, and influence the thermodynamic and transport properties of the hosts. Since many experiments and almost all technical applications are **not** performed at low temperatures the magnetic impurities are generally far above their Kondo temperature  $T_K$  and show their full magnetic behavior. The theoretical investigation of the magnetic state has been explored in much less detail than the Kondo ground state for spin 1/2 impurities.

In many cases the Kondo temperature is very low, in the range of liquid helium temperature. In this case the impurity is in the magnetic state at relatively low temperature. (The word impurity is in this paper reserved to impurities which possess - at sufficiently high temperature - a magnetic moment). When the temperature is several times the Kondo temperature one is sufficiently above  $T_K$  to destroy the Kondo ground state. On the other hand one may expect that the properties of the magnetic state are not yet influenced by the thermal excitations due to the finite temperature. Therefore a number of theoretical investigations treat the magnetic state at zero temperature, i.e. as a magnetic ground state. This approach is probably justified but it leaves the work always vulnerable to the criticism that there is no magnetic moment at zero temperature.

Therefore in this paper I prefer to use the effect of a magnetic field on the Kondo state. A magnetic field which is an order of magnitude larger than  $k_B T_K / \mu_B$  ( $\mu_B$ =Bohr magneton) destroys the Kondo singlet state as well and yields the magnetic state. Its side effects are that it changes the energy of the d-states by  $\pm \mu_B B$  and shifts the conduction bands by  $\pm \mu_B B$ . The latter yields the Pauli susceptibility but has otherwise only a negligible effect on the interaction between the impurity and the conduction electrons because the Fermi level for spin-up and down electrons readjusts to the same height (as before).

Friedel [1] and Anderson [2] derived a criterion for the instability of the paramagnetic state, i.e. the formation of a magnetic moment: Take the density of states  $N_d(\varepsilon_F)$  of the d-resonance at the Fermi energy (in the paramagnetic state) and multiply it by the Coulomb repulsion energy  $U$ . If the product  $N_d U > 1$  then a magnetic moment is formed. Within

mean field theory the d-density of states is given by a Lorentz function

$$N_{d,\sigma}(\varepsilon) = \frac{1}{\pi} \frac{\Gamma_{mf}}{(\varepsilon - E_{d,\sigma})^2 + \Gamma_{mf}^2}$$

where  $E_{d,\sigma}$  is an effective energy of the d-electrons in the spin-up or down state,  $E_{d,\sigma} = E_d + U \langle n_{d,-\sigma} \rangle$  while  $\langle n_{d,-\sigma} \rangle$  is the average occupation of the d-electron with the opposite spin) and the resonance width  $\Gamma_{mf}$  is given in mean field theory by

$$\Gamma_{mf} = \pi |V_{sd}|^2 N_s$$

Here  $V_{sd}$  is the s-d-hopping matrix element between a conduction electron and the d-state at the impurity and  $N_s$  is the density of states of the conduction electrons. In the mean field theory an occupied  $d_{\uparrow}^{\dagger}$  electron state can only make transitions into  $c_{\mathbf{k}\uparrow}^{\dagger}$ -states. (Throughout this paper I express electron states by their creation operators).

It is well known that the mean field theory has a number of shortcomings. During the last few years the group of the author has developed a new approach to the impurity problem, in particular the Friedel-Anderson and the Kondo impurity. In this **FAIR** method a **F**riedel state is **A**rtificially built from each conduction band and **I**nserted as a **R**esonance state into the conduction or s-band of spin-up and spin-down electrons. In the appendix a short review of the FAIR solution for the Friedel impurity is sketched.

The FAIR solution for the magnetic state yields a considerably lower energy for the "magnetic ground state" and requires a much larger critical Coulomb interaction to form a magnetic state. This is of some practical importance since the mean field approximation is used in a number of numerical spin-density functional theory calculations for the magnetic moment of impurities in an (s,p) metal host [14], [15], [16], [17], [18].

In addition to the size of the magnetic moment one would like to know the density of states in the magnetic state. The answer of the mean field theory has been discussed above. But there have been a number of suggestions that the d-resonance is broader than the mean field suggests (see for example Logan [19]). The mean field theory decouples the spin-up d-electron from the spin-down d-electron, but in reality the d-electrons are coupled through the Coulomb energy. A transition in the  $d_{\uparrow}^{\dagger}$  electron state changes the energy and the state of the  $d_{\downarrow}^{\dagger}$  electron as well. Therefore it has been suggested in the past that the d-resonances in the Friedel-Anderson impurity are larger than the mean field theory predicts. A wider d-resonance in the Friedel-Anderson impurity together with the condition  $N_d U > 1$  would require a larger Coulomb energy to form a magnetic moment. In this connection the previous result of the author that the FAIR solution requires a (two times) larger Coulomb energy to form a magnetic moment would find a simple physical interpretation.

It is the goal of this paper to calculate the density of states of the "magnetic ground state" in the FAIR solution and compare it with the mean field density of states. In section II the theoretical background of the magnetic state of the Friedel-Anderson impurity is sketched. In section III electrons and holes are introduced into the magnetic ground state. Their interactions and excitation energies are derived. In section IV the results of the numerical

calculations are presented. Finally in section V and VI the results are discussed together with the conclusion. In the appendix A the basic idea of the FAIR method is sketched.

## 2 Theoretical Background

The simplified Hamiltonian for a magnetic impurity is generally described by the Friedel-Anderson (FA) Hamiltonian

$$H_{FA} = \sum_{\sigma} \left\{ \sum_{\nu=0}^{N-1} \varepsilon_{\nu} c_{\nu\sigma}^{\dagger} c_{\nu\sigma} + E_d d_{\sigma}^{\dagger} d_{\sigma} + \sum_{\nu=0}^{N-1} V_{\nu}^{sd} [d_{\sigma}^{\dagger} c_{\nu\sigma} + c_{\nu\sigma}^{\dagger} d_{\sigma}] \right\} + U n_{d\uparrow} n_{d\downarrow} \quad (1)$$

Here the operators  $c_{\nu\sigma}^{\dagger}$  represent s-electrons, i.e. the conduction band.

### 2.1 The FAIR method

In the Friedel-Anderson Hamiltonian in equ. (1) the d-state for each spin interacts with every electron in the conduction band. Imagine how much easier the task would be if the d-electron would interact only with a single electron state (in each spin band). All other conduction band states would represent just a background or quasi-vacuum. This is the FAIR approach.

During the last few years the author introduced such a solution to the Friedel-Anderson impurity problem in which only four electron states, the spin-up and spin-down d-states  $d_{\uparrow}^{\dagger}$  and  $d_{\downarrow}^{\dagger}$  and two FAIR states,  $a_{0\uparrow}^{\dagger}$  and  $b_{0\downarrow}^{\dagger}$  interact through the Coulomb and s-d-hopping potential. These states  $a_{0\uparrow}^{\dagger}$  and  $b_{0\downarrow}^{\dagger}$  are composed of the spin-up and spin-down conduction band states. They are the Friedel Artificially Inserted Resonance states or FAIR states. The interaction of the remaining conduction electron states with the d-states is insignificant; they just yield a background. This yields very good ground-state properties. The FAIR states are composed of the corresponding conduction bands

$$a_{0\uparrow} = \sum_{\nu=0}^{N-1} \alpha_0^{\nu} c_{\nu\uparrow} \quad b_{0\downarrow} = \sum_{\nu=0}^{N-1} \beta_0^{\nu} c_{\nu\downarrow}$$

The remaining  $(N - 1)$  states in each spin band are constructed orthogonal to the corresponding FAIR state, orthonormal to each other and sub-diagonal with respect to the band energy Hamiltonian

$$H_0 = \sum_{\nu=0}^{N-1} \varepsilon_{\nu} c_{\nu\sigma}^{\dagger} c_{\nu\sigma}$$

This yields new bases for the conduction bands  $\{a_{i,\uparrow}^{\dagger}\}$  and  $\{b_{i,\downarrow}^{\dagger}\}$  with  $1 \leq i \leq (N - 1)$ . These new bases are uniquely determined by the two FAIR states.

Within the new bases the FA-Hamiltonian (1) can be expressed as

$$H_{FA} = H'_0 + H'_1$$

with

$$\begin{aligned} H'_0 &= H'_{0,\uparrow} + H'_{0,\downarrow} + U n_{d\uparrow} n_{d\downarrow} \\ H'_1 &= H'_{1,\uparrow} + H'_{1,\downarrow} \end{aligned}$$

where

$$H'_{0,\uparrow} = \sum_{i=1}^{N-1} E_i^{(a)} a_{i,\uparrow}^\dagger a_{i,\uparrow} + E_0^{(a)} a_{0,\uparrow}^\dagger a_{0,\uparrow} + E_d d_{\uparrow}^\dagger d_{\uparrow} + V_0^{(a)sd} \left[ a_{0,\uparrow}^\dagger d_{\uparrow} + d_{\uparrow}^\dagger a_{0,\uparrow} \right] \quad (2)$$

$$H'_{1,\uparrow} = \sum_{i=1}^{N-1} V_i^{(a)fr} \left[ a_{0,\uparrow}^\dagger a_{i,\uparrow} + a_{i,\uparrow}^\dagger a_{0,\uparrow} \right] + \sum_{i=1}^{N-1} V_i^{(a)sd} \left[ d_{\uparrow}^\dagger a_{i,\uparrow} + a_{i,\uparrow}^\dagger d_{\uparrow} \right] \quad (3)$$

and the spin-down Hamiltonians are obtained by replacing  $\uparrow$  by  $\downarrow$  and the  $a_i^\dagger$ -states by  $b_i^\dagger$ -states.

### 2.1.1 Nest states

The Hamiltonian  $H'_0$  is diagonal in the band states  $a_{i,\uparrow}^\dagger$  and  $b_{i,\downarrow}^\dagger$  for  $0 < i < N - 1$ . The only interaction takes place between the states  $a_{0,\uparrow}^\dagger$ ,  $d_{\uparrow}$ ,  $b_{0,\downarrow}$  and  $d_{\downarrow}$ . I call these states the **nest states**. The ground state of the Hamiltonian  $H'_0$  is straight forward. It consists of the coupled state between the nest states and a partially occupied spin-up and down band. I occupy each spin component with  $N/2$  electrons, putting  $n = N/2 - 1$  electrons into each conduction band states and one spin-up and one spin-down electron into the nest. This yields the magnetic ground state as described in equ. (4).

$$\Psi_{MS} = \left[ A_{a,b} a_{0\uparrow}^\dagger b_{0\downarrow}^\dagger + A_{a,d} a_{0\uparrow}^\dagger d_{\downarrow}^\dagger + A_{d,b} d_{\uparrow}^\dagger b_{0\downarrow}^\dagger + A_{d,d} d_{\uparrow}^\dagger d_{\downarrow}^\dagger \right] |\mathbf{0}_{a,\uparrow} \mathbf{0}_{b,\downarrow}\rangle \quad (4)$$

where  $|\mathbf{0}_{a,\uparrow} \mathbf{0}_{b,\downarrow}\rangle = \prod_{j=1}^{n-1} a_{j\uparrow}^\dagger \prod_{j=1}^{n-1} b_{j\downarrow}^\dagger |\Phi_0\rangle$  represents a kind of quasi-vacuum ( $n = N/2$ ).

The calculation of the coefficients  $A_{a,b}, \dots$  yields a secular Hamiltonian  $H_{1/1}^{nst}$  which I call the nest-Hamiltonian and which has the form

$$H_{1/1}^{nst} = \begin{pmatrix} E_0^{(a)} + E_0^{(b)} & V_b^{sd} & V_a^{sd} & 0 \\ V_b^{sd} & E_0^{(a)} + E_d & 0 & V_a^{sd} \\ V_a^{sd} & 0 & E_d + E_0^{(b)} & V_b^{sd} \\ 0 & V_a^{sd} & V_b^{sd} & 2E_d + U \end{pmatrix}$$

Here the abbreviations are used:  $V_a^{sd} = V_0^{(a)sd}$  and  $V_b^{sd} = V_0^{(b)sd}$  (see equ.(2)). The superscript *nst* stands for nest and the subscript 1/1 gives the number of nest electrons in the spin-up and spin-down state. (The energy of the occupied band states is not included. It yields

the same contribution to each component).  $H_{1/1}^{nst}$  has four eigenvalues and eigenstates. The lowest eigenvalue yields the ground state. The components of the ground state, nest plus the band states, are shown in Fig.1.

The first order correction to the energy, i.e. the expectation value of  $H'_1$  is zero. But in addition the second order perturbation of  $H'_1$  is extremely small. This is demonstrated in appendix B.

It may appear remarkable that the neglect of the interactions between the d-electron and all the band states  $\{a_{j,\uparrow}^\dagger\}$  and  $\{b_{j,\downarrow}^\dagger\}$  yields a realistic ground state. But it is not unheard off that one can obtain an excellent ground state while neglecting a major part of the interaction in the system. The BCS theory is a good example because it only includes the electron-phonon interaction between Cooper pairs of time-reversed electrons. The interaction between all the other electrons is neglected although their number is much larger.

One major part of the numerical calculation is, of course, the optimization of the two FAIR states  $a_{0,\uparrow}^\dagger$  and  $b_{0,\downarrow}^\dagger$  so that the expectation value of the energy  $E_{00} = \langle \Psi_{MS} | H'_0 | \Psi_{MS} \rangle$  of the Hamiltonian  $H'_0$  has a minimum. The optimization procedure is described at length in previous papers [20], [21], [22] and is taken for granted in this paper and will not be described here. (The FAIR states are rotated in Hilbert space). Since we don't count the FAIR states any more as band states the number of band states is reduced by one and their energy is slightly shifted (by less than the original energy spacing). The band states enter in the energy  $E_{00}$  only through the kinetic (band) energy of the occupied band states. In a way they just prepare the nest for the states  $[a_{0,\uparrow}^\dagger, d_\uparrow, b_{0,\downarrow}^\dagger, d_\downarrow]$ .

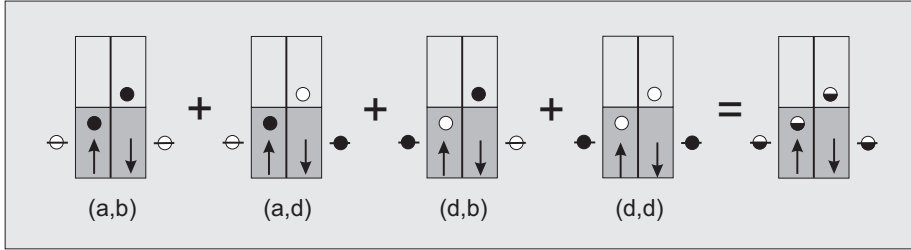


Fig.1: The composition of the magnetic state  $\Psi_{MS}$  in the nest is shown.

It consists of four Slater states. Each Slater state has a half-full spin-up and down band, two FAIR states (circles in within the bands) and two d-states (circles on the left and right of the band). Full black circles represent occupied states and light grey represent empty states. The band at the right with the half-filled circles symbolizes the magnetic solution with four Slater states.

In the numerical calculation we will present the results for two examples with the parameters  $U = 1.0$ ,  $E_d = -0.5$  and  $|V_{sd}^0|^2 = 0.05$  and  $|V_{sd}^0|^2 = 0.025$ . The smaller value of the s-d-matrix element permits a better fit of the resulting resonance curve with a Lorentz curve since the effect of the finite width of the band is smaller.

### 2.1.2 Self-consistent perturbation

In the construction of the magnetic ground state  $\Psi_{MS}$  the Hamiltonian  $H'_1$  has been completely neglected. Below we will derive the excitation energies by introducing an additional electron (hole) into an empty (occupied) states. For this calculation it is important to know whether the empty state is really empty or whether transitions from the ground state into the state due to  $H'_1$  have partially occupied this state. (This problem is well known from the calculation of the electron-phonon mass enhancement. In the calculation of the electron-phonon self-energy one injects an electron into an "empty state"  $\mathbf{k}$  above the Fermi energy. The transitions of this electron via the electron-phonon interaction into other empty states  $\mathbf{k}'$  contribute to the self-energy  $\Sigma$ . However, the state  $\mathbf{k}$  was not really empty because transitions from the ground state into  $\mathbf{k}$  already created a finite occupation of  $\mathbf{k}$ . One has to correct the self-energy due to these processes).

In the appendix I show that transitions from the ground state into empty band states (due to  $H'_1$ ) are practically zero. The interference between transitions from the d-state and from the corresponding FAIR state almost perfectly cancel each other. The total weight in all perturbation states is only of the order of  $10^{-4}$  and can be completely neglected. Therefore the band states are either completely empty or fully occupied.

## 3 Calculation of Excitations

### 3.1 Injection of an electron

In Fig.2 a spin-up electron is injected into one of the empty states  $a_{j\uparrow}^\dagger$  of the  $\{a_{\uparrow}^\dagger\}$ -band. This yields the Slater states ( $\alpha$ ). The Slater state ( $\beta$ ) is obtained by injecting an electron into the nest, either into the state  $a_{0\uparrow}^\dagger$  or  $d_{\uparrow}^\dagger$ .

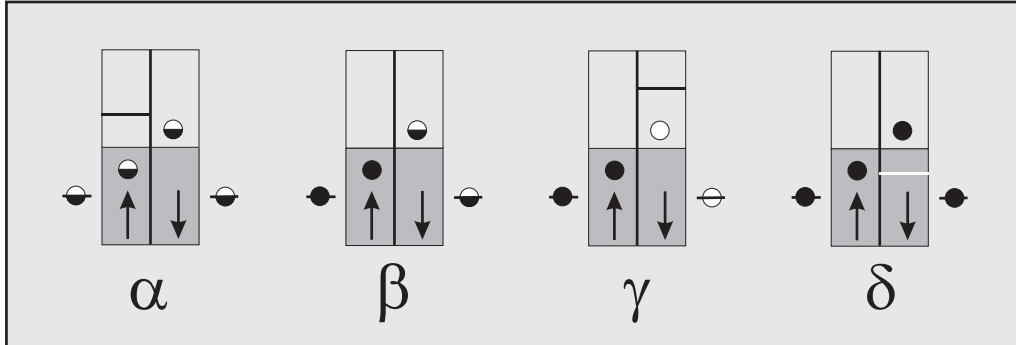


Fig.2: An electron has been injected into the spin-up band and the spin up nest. This induces electron or hole transitions in the spin-down band. The resulting Slater states are shown as ( $\gamma$ ) and ( $\delta$ ). (Each band with half circles consists of two Slater states.)

The injection into  $a_{0\uparrow}^\dagger$  or  $d_{\uparrow}^\dagger$  yields

$$\begin{aligned} a_{0\uparrow}^\dagger \Psi_{MS} &= \left( A_{d,b} a_0^\dagger d_{\uparrow}^\dagger b_{0\downarrow}^\dagger + A_{d,d} a_0^\dagger d_{\uparrow}^\dagger d_{\downarrow}^\dagger \right) |\mathbf{0}_{a,\uparrow} \mathbf{0}_{b,\downarrow}\rangle \quad \text{for } a_0^\dagger \\ d_{\uparrow}^\dagger \Psi_{MS} &= - \left( A_{a,b} a_{0\uparrow}^\dagger d_{\uparrow}^\dagger b_{0\downarrow}^\dagger + A_{a,d} a_{0\uparrow}^\dagger d_{\uparrow}^\dagger d_{\downarrow}^\dagger \right) |\mathbf{0}_{a,\uparrow} \mathbf{0}_{b,\downarrow}\rangle \quad \text{for } d_{\uparrow}^\dagger \end{aligned} \quad (5)$$

Both final states yield a double occupancy of the spin up nest states. Furthermore these states are not eigenstates of the nest. With respect to the (basis) states  $a_0^\dagger d_{\uparrow}^\dagger b_{0\downarrow}^\dagger |\mathbf{0}_{a,\uparrow} \mathbf{0}_{b,\downarrow}\rangle$  and  $a_0^\dagger d_{\uparrow}^\dagger d_{\downarrow}^\dagger |\mathbf{0}_{a,\uparrow} \mathbf{0}_{b,\downarrow}\rangle$  the nest Hamiltonian takes the form

$$H_{2/1}^{nst} = \begin{pmatrix} \left( E_d + E_0^{(a)} \right) + E_0^{(b)} & V_b^{sd} \\ V_b^{sd} & \left( E_d + E_0^{(a)} \right) + E_d + U \end{pmatrix} \quad (6)$$

By diagonalization one obtains the eigenstates  $\Psi_{2/1}^{(1)}$  and  $\Psi_{2/1}^{(2)}$  with

$$\Psi_{2/1}^{(\alpha)} = a_{0\uparrow}^\dagger d_{\uparrow}^\dagger \left( B_{b\downarrow}^{(\alpha)} b_{0\downarrow}^\dagger + B_{d\downarrow}^{(\alpha)} d_{\downarrow}^\dagger \right) |\mathbf{0}_{a,\uparrow} \mathbf{0}_{b,\downarrow}\rangle \quad (7)$$

The states  $(\alpha)$  and  $(\beta)$  in Fig.2 are the initial states which one obtains through injection of a spin-up electron into the ground state. Due to the perturbation Hamiltonian  $H'_1$  these states interact with each other and  $(\beta)$  interacts with the states  $(\gamma)$  and  $(\delta)$ .

In table I the possible states which can be obtained through the injection of a spin-up electron plus linear coupling through  $H'_1$  are collected. These states are  $(\alpha)$  the two-electron nest ground state plus one electron,  $(\beta)$  a nest with two spin-up and one spin-down electron,  $(\gamma)$  a full spin-up and empty spin-down nest plus one spin down electron and  $(\delta)$  a full spin-up and full spin-down nest and one spin down hole. In table I these states, their number and their energies are listed.

$\Psi_f$	number	energy	
$a_{j\uparrow}^\dagger \Psi_{MS}$	$N/2$	$E_j^{(a)}$	
$\Psi_{2/1}^{(\alpha)}$	$2, \alpha = 1, 2$	$E_d + E_0^{(a)} + E_{2/1}^\alpha - E_{00}$	
$a_{0\uparrow}^\dagger d_{\uparrow}^\dagger b_{j\downarrow}^\dagger  \mathbf{0}_{a,\uparrow} \mathbf{0}_{b,\downarrow}\rangle$	$N/2$	$E_d + E_0^{(a)} + E_j^{(b)} - E_{00}$	
$b_{k\downarrow} a_{0\uparrow}^\dagger d_{\uparrow}^\dagger b_{0\downarrow}^\dagger d_{\downarrow}^\dagger  \mathbf{0}_{a,\uparrow} \mathbf{0}_{b,\downarrow}\rangle$	$N/2 - 1$	$2E_d + U + E_0^{(a)} + E_0^{(b)} - E_k^{(b)} - E_{00}$	

Table I: This table describes the states of Fig.2 which are generated by the injection of one spin-up electron into the magnetic ground state and transition from the resulting states through  $H'_1$ . The state  $\Psi_{MS}$  is given by equ. (4) and  $\Psi_{2/1}^{(\alpha)}$  is given by (7). The energy is measured from the ground-state energy  $E_{00}$ .

Fig.2 and table I show all the spin-up electron excitations which interact linearly in  $H'_1$ . This is a total of  $(\frac{3}{2}N + 1)$  states. It is straight forward to construct the secular matrix (i.e.



the excitation Hamiltonian  $H^{xct}$ ) between the excitations in table I. One may put the two nest states  $\Psi_{2/1}^{(1)}$  and  $\Psi_{2/1}^{(2)}$  at the positions one and two, followed by the  $(\frac{3}{2}N - 1)$  additional single particle excitations. We denote these  $(\frac{3}{2}N + 1)$  states as  $\varphi_\nu$ . The diagonal of the Hamiltonian is given by the energies in table I. The off-diagonal elements of  $H^{xct}$  are the matrix elements of  $H'_1$  between the states  $(\alpha, \beta, \gamma, \delta)$  in Fig.2. The single particle excitations interact only with the first two nest states through  $H'_1$  but not among each other. (In appendix B the corresponding matrix elements are shown in table III for similar transitions from the ground state.)

This Hamiltonian  $H^{xct}$  is diagonalized and yields a set of  $(\frac{3}{2}N + 1)$  new eigenstates  $\psi_\mu$  with eigenenergies  $E_\mu^{xct}$ . The components of the eigenstates  $\psi_\mu$  in terms of  $\varphi_\nu$  are given as columns  $(\psi_\mu^\nu)$ . The  $\nu$ th row of the matrix  $(\psi_\mu^\nu)$  yields the amplitude of our  $\nu$ th original state  $\varphi_\nu$  in terms of the new eigenstates  $\psi_\mu$ . If this  $\nu$ th original state is, for example,  $a_{j\uparrow}^\dagger \Psi_{MS}$  then it can be expressed in the new eigenstates as

$$\varphi_\nu = a_{j\uparrow}^\dagger \Psi_{MS} = \sum_\mu \psi_\mu^\nu \psi_\mu$$

Its density of states is then

$$N_\nu(\varepsilon) = \sum_\mu |\psi_\mu^\nu|^2 \delta(\varepsilon - E_\mu^{xct})$$

Since electron injection creates only the states  $(\alpha)$  and  $(\beta)$  one obtains the full (spin-up) excitation spectrum by summing over these  $(\frac{1}{2}N + 2)$  states. The weight of states  $a_{j\uparrow}^\dagger \Psi_{MS}$  is one, however, the weight of  $a_{0\uparrow}^\dagger \Psi_{MS}$  is only  $|A_{d,b}|^2 + |A_{d,d}|^2$  since

$$\begin{aligned} & a_{0\uparrow}^\dagger \left[ A_{a,b} a_{0\uparrow}^\dagger b_{0\downarrow}^\dagger + A_{a,d} a_{0\uparrow}^\dagger d_{\downarrow}^\dagger + A_{d,b} d_{\uparrow}^\dagger b_{0\downarrow}^\dagger + A_{d,d} d_{\uparrow}^\dagger d_{\downarrow}^\dagger \right] |\mathbf{0}_{a,\uparrow} \mathbf{0}_{b,\downarrow}\rangle \\ &= \left[ A_{d,b} a_{0\uparrow}^\dagger d_{\uparrow}^\dagger b_{0\downarrow}^\dagger + A_{d,d} a_{0\uparrow}^\dagger d_{\uparrow}^\dagger d_{\downarrow}^\dagger \right] |\mathbf{0}_{a,\uparrow} \mathbf{0}_{b,\downarrow}\rangle \end{aligned}$$

A similar result is found for the weight of  $d_{\uparrow}^\dagger \Psi_{MS}$  which is  $|A_{a,b}|^2 + |A_{a,d}|^2$ .

Since  $a_{0\uparrow}^\dagger \Psi_{MS}$  and  $d_{\uparrow}^\dagger \Psi_{MS}$  are not eigenstates of  $H'_0$  they represent a combination of the two eigenstates  $\Psi_{2/1}^{(\alpha)}$ . In Fig.3 is sketched what happens when an electron is injected into either the state  $a_{0\uparrow}^\dagger$  or  $d_{\uparrow}^\dagger$ . The electron injection yields a superposition of the two eigenstates  $\Psi_{2/1}^{(\alpha)}$ . From these states the electron can make a transition into any of the  $(\gamma)$  states via  $H'_1$ . The two transition amplitudes interfere in this transition. This interference has to be included in the calculation of the spectral weight density of  $a_{0\uparrow}^\dagger \Psi_{MS}$  and  $d_{\uparrow}^\dagger \Psi_{MS}$  (which requires just the scalar products between  $a_{0\uparrow}^\dagger \Psi_{MS}$  and  $\Psi_{2/1}^{(\alpha)}$  (or  $d_{\uparrow}^\dagger \Psi_{MS}$  and  $\Psi_{2/1}^{(\alpha)}$ ). This is discussed in more detail in appendix C.

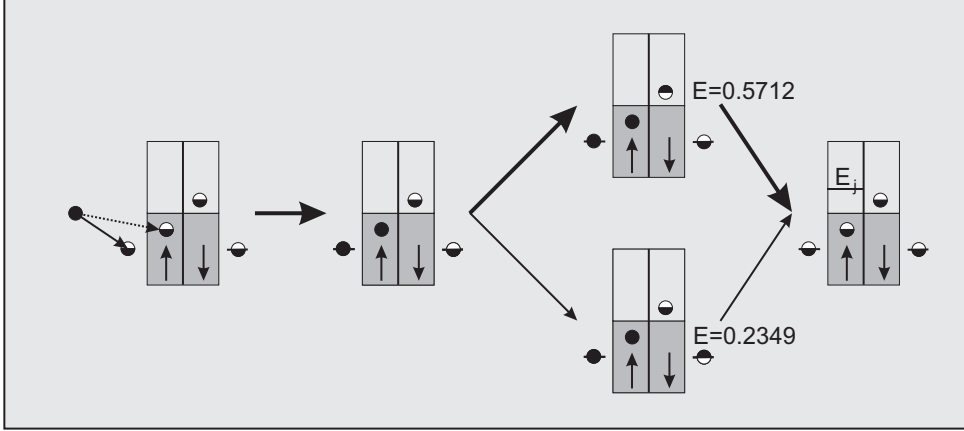


Fig.3: An electron has been injected into the  $a_{0\uparrow}^\dagger$  state (or  $d_{\uparrow}^\dagger$  state, dashed arrow). The resulting state is a superposition of two nest states. From these nest states the electron makes (as one possibility) a transition into the state  $a_{j\uparrow}^\dagger$  where the two amplitudes interfere. The energies of the two nest states are shown. The different thickness of the arrows shows different probabilities for the two paths.

### 3.2 Injection of a hole

For the full spectrum of excitations one has to include the injection of holes into the occupied states. This is shown in Fig.4. The hole can be injected into the occupied states  $a_{j\uparrow}^\dagger$  yielding  $a_{j\uparrow}\Psi_{MS}$  or into the nest. In the latter case the spin-up part of the nest is emptied. This yields for the secular matrix of the nest in analogy to equ. (6)

$$H_{0/1}^{nst} = \begin{pmatrix} E_0^{(b)} & V_b^{sd} \\ V_b^{sd} & E_d \end{pmatrix} \quad (8)$$

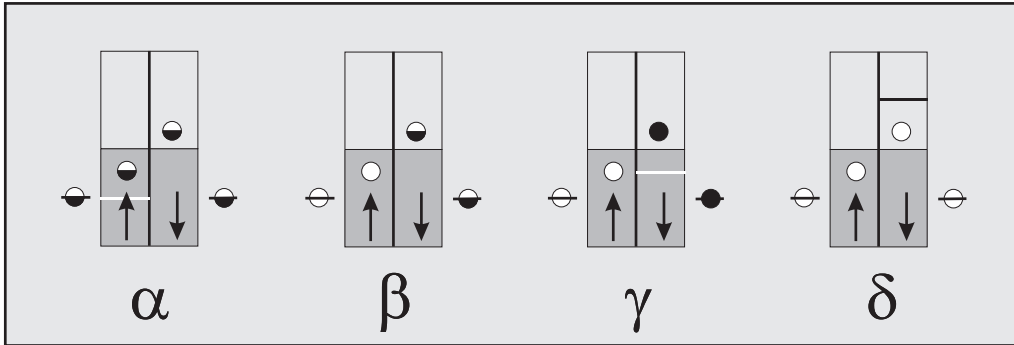


Fig.4: An hole has been injected into the spin-up band and the spin up nest. This induces electron or hole transitions in the spin-down band. The resulting Slater states are shown as ( $\gamma$ ) and ( $\delta$ ).

state	number	energy
$a_{j\uparrow}\Psi_{MS}$	$N/2 - 1$	$-E_j^{(a)} =  E_j^{(a)} $
$\Psi_{\downarrow}^{(\alpha)} = \left(B_b b_{0\downarrow}^{\dagger} + B_d d_{\downarrow}^{\dagger}\right)  \mathbf{0}_{a,\uparrow}\mathbf{0}_{b,\downarrow}\rangle$	$2, \alpha = 1, 2$	$E_{\downarrow}^{(\alpha)} - E_{00}$
$b_{j\downarrow} b_{0\downarrow}^{\dagger} d_{\downarrow}^{\dagger}  \mathbf{0}_{a,\uparrow}\mathbf{0}_{b,\downarrow}\rangle$	$N/2 - 1$	$E_d + E_0^{(b)} - E_j^{(b)} - E_{00}$
$b_{j\downarrow}^{\dagger}  \mathbf{0}_{a,\uparrow}\mathbf{0}_{b,\downarrow}\rangle$	$N/2$	$E_j^{(b)} - E_{00}$

Table II: This table describes the states of Fig.4 which are generated by the injection of one spin-up hole into the magnetic ground state and transition from the resulting states through  $H'_1$ . The energy is measured from the ground-state energy  $E_{00}$ .

The construction of the excitation or secular Hamiltonian  $H^{xct}$  is in complete analogy to the electron injection. This time the number of excitations is  $\frac{3}{2}N$ . The spectrum is obtained in the same way as before.

## 4 Numerical Results

For the numerical calculation a conduction band with a finite number of states is used. We follow here Wilson [23] by using an s-electron band with constant density of states and the Fermi level in the center, which we divide into energy cells  $\mathfrak{E}_{\nu}$ . In each energy cell (which may contain  $Z_{\nu}$   $\mathbf{k}$ -states  $c_{\mathbf{k}}^{\dagger}$ ) we rearrange the states (by an orthogonal transformation) so that one state  $c_{\nu}^{\dagger} = Z_{\nu}^{-1/2} \sum_{\mathbf{k}} c_{\mathbf{k}}^{\dagger}$  accumulates all the interaction with the d-states while the other  $(Z_{\nu} - 1)$  states have zero interaction with the d-states. Wilson normalized the energy in terms of the Fermi energy so that his band extended from  $-1$  to  $1$ . Wilson's logarithmic scale for the energy cells is not opportune for the present investigation because it is not fine enough at the energy of the d-resonance. Therefore I use a linear sub-division of the energy band  $(-1 : 1)$ . For the majority of calculations the energy band is sub-divided into  $N = 40, 80$  and  $160$  energy cells. The state  $c_{\nu}^{\dagger}$  represents all the s-electron states in the cell  $\mathfrak{E}_{\nu} = (-1 + \nu \frac{2}{N} : -1 + (\nu + 1) \frac{2}{N})$  and possesses the average energy  $\varepsilon_{\nu} = -1 + (\nu + \frac{1}{2}) \frac{2}{N}$  (corresponding to  $-.975, -.925, \dots, .975$  for  $N = 40$ ). For  $N$  energy cells with constant width of  $2/N$  the s-d-matrix elements  $V_{\nu}^{sd}$  is given by  $V_{sd}^0/\sqrt{N}$  so that  $\sum_{\nu} |V_{\nu}^{sd}|^2 = |V_{sd}^0|^2$ .

In the following I show the results for the Friedel-Anderson Hamiltonian with the d-level energy  $E_d = -0.5$ , the Coulomb energy  $U = 1.0$  and an s-d-hopping matrix element of  $|V_{sd}^0|^2 = 0.025$ . The magnetic moment of this impurity is  $\mu = 0.998\mu_B$  (for  $N = 80$ ). The calculations are performed with  $N = 40, 80$  or  $160$  energy levels of constant spacing. A second set of results is derived for the parameters  $E_d = -0.5$ ,  $U = 1$  and  $|V_{sd}^0|^2 = 0.05$ .

To assure that the magnetic state  $\Psi_{MS}$  is indeed the ground state (i.e. to prevent the formation of a singlet state) a magnetic field  $B$  is applied yielding a magnetic energy  $E_B = \mu_B B$ . This energy is chosen so that  $E_B > 10k_B T_K$ . I estimate the Kondo energy from the difference between the energies of the singlet and the triplet state. This energy difference

is about  $8 \times 10^{-4}$  for  $|V_{sd}^0|^2 = 0.05$  and of the order of  $10^{-7}$  for  $|V_{sd}^0|^2 = 0.025$ . It turned out that the required magnetic energy is in both cases so small that it yields no noticeable changes. This is partly due to the fact that the absolute smallest band energies which are  $\pm 1/N$  act as a finite temperature as Wilson pointed out [23]. For  $N = 40$  this corresponds to a temperature of  $\varepsilon_F/40$  which is a very large temperature compared with most Kondo temperatures. But magnetic field is of academic importance to assure the magnetic state  $\Psi_{MS}$  is the appropriate ground state.

The use of equidistant energy levels is important to identify the resonance state within the electron bands. But it has the drawback that it does not describe well the behavior of the wave function at low energies. At low energies the logarithmic energy scale which Wilson introduced would be more appropriate. But the evaluation of the density of states is much more difficult for a non-linear energy scale.

For each spin band one obtains a spectrum with a total weight of  $(N + 1)$ , corresponding to  $N$  s-electron states and one d-electron state. However, the number of energy levels is  $(3N + 1)$ . (This is the number of eigenstates of the excitation Hamiltonians for electrons and holes together). This means that the weight at the individual energies is at least for  $2N$  energies much less than one. In Fig.5 the spectral weight at different energies is shown in the energy range from  $-1$  to  $+1$  for the minority band. For negative energies the weight is either very close to one or very small. Here one can calculate the density of states by the separation of the levels with weight close to one (by dividing the weight by the level separation). The evaluation is more complicated for positive energies. However, here the sum of neighboring energy levels is close to one. Then one can calculate the "center of weight" for two neighboring levels which have a total weight close to one and then proceed as before. It turns out that the best approach is to start from the lower and upper ends of the band in the evaluation.

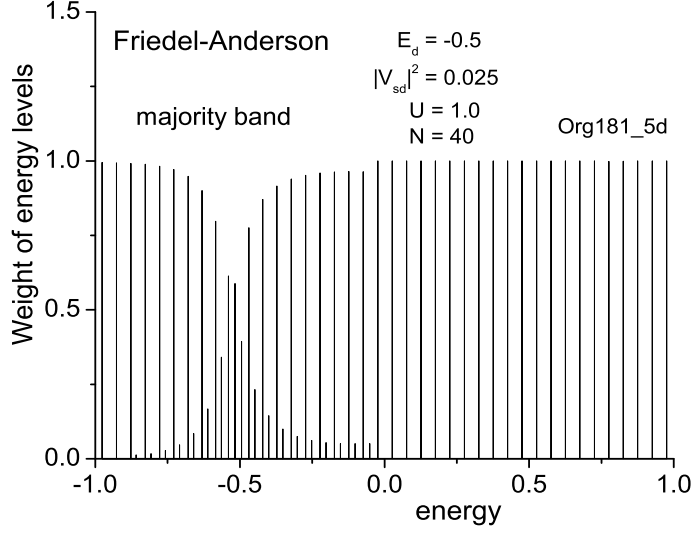


Fig.5: The spectral weight for the different excitation energies.

In Fig.6a the density of states of the excitation spectrum for the majority spin is shown. The full circles are obtained with  $N = 40$  states and the stars use  $N = 80$  equally spaced Wilson states. The full curve represents a Lorentz curve with the parameters

$$N_d(\varepsilon) = \frac{1}{\pi} \frac{0.08}{(\varepsilon - (-0.53))^2 + 0.08^2}$$

The resonance energy is  $E_r = -0.53$  and the resonance (half) width is  $\Gamma_r = 0.08$ . The corresponding mean field resonance width is  $\Gamma_{mf} = 0.039$ .

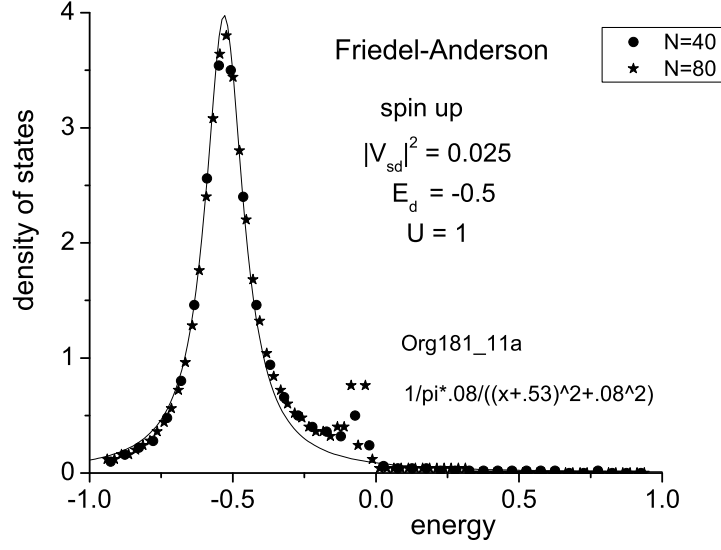


Fig.6a: The density of states for the majority spins. The full circles are calculated with  $N = 40$  states and the stars use  $N = 80$  equally spaced Wilson states. The full curve represents a Lorentz curve with the resonance energy  $E_r = -0.53$  and the width  $\Gamma_r = 0.08$ . This width is twice the mean-field value of  $\Gamma_{mf} = 0.039$ .

In Fig.6b the density of states of the minority spin is drawn. Again the full curve represents a Lorentz curve with the resonance at  $E_r = 0.52$  and a resonance half-width of  $\Gamma_r = 0.8$ .

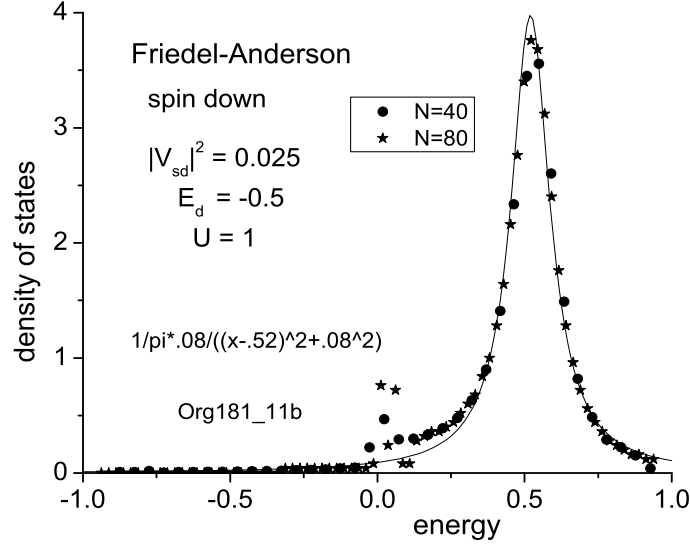


Fig.6b: The density of states for the minority spins. The full circles are calculated with  $N = 40$  states and the stars use  $N = 80$  equally spaced Wilson states. The full curve represents a Lorentz curve with the resonance energy  $E_r = 0.52$  and the width  $\Gamma_r = 0.08$ . Again this width is twice the mean-field value of  $\Gamma_{mf} = 0.039$ .

For comparison Fig.7 shows the result of a similar calculation and evaluation for a simple Friedel resonance, where the Coulomb energy  $U$  is set equal to zero. The evaluation yields a Lorentz curve with  $E_r = -0.51$  and  $\Gamma_r = 0.044$ . The s-d-matrix element is still given by  $|V_{sd}^0|^2 = 0.025$ .

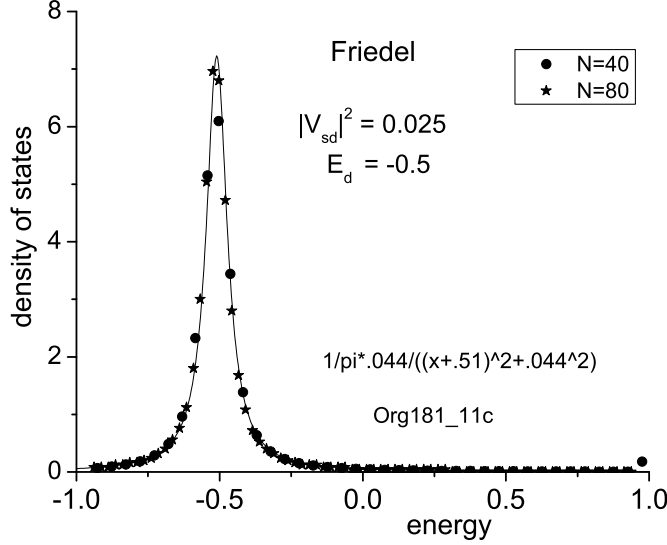


Fig.7: The density of states for an impurity with  $U = 0$ . The full circles and the stars are calculated with  $N = 40$  and  $N = 80$  states. The full curve represents a Lorentz curve with the resonance energy  $E_r = -0.51$  and the width  $\Gamma_r = 0.044$ .

Alternatively we tried to obtain the density of states by broadening the  $\delta$ -shaped energy spectrum in Fig.5 with a Gaussian curve  $\sqrt{1/2\pi} \exp [(\varepsilon - E_d)^2 / 2\sigma^2]$ . This method worked quite well. The optimal density curve was obtained when  $\sqrt{2}\sigma$  was equal to the level distance  $2/N$ . The width of the two resonances was essentially the same as in Fig.6a,b and Fig.8a,b. Only the heights were slightly reduced. However, I prefer to use the other evaluation method in this paper so that there is no doubt that the broadening of the resonance width is a real physical effect and not due to an artificial broadening with a Gaussian curve.

In a second series the majority and minority density of states have been calculated for the parameters  $E_d = -0.5$ ,  $U = 1$ , and  $|V_{sd}^0|^2 = 0.05$ . This impurity possesses a magnetic moment of  $\mu = 0.997\mu_B$ . In this case the mean-field theory yields a resonance width of  $\Gamma_{mf}=0.079$ . The best fit to the numerical results yields  $\Gamma_{FAIR} = 0.17$ . It is again about twice the value of the mean field. (The resonance curves are no longer perfectly symmetrical because of the finite width of the conduction band).

The corresponding Friedel density of states (which is not shown here) has a resonance



with of 0.08 which is quite close to the theoretical value of 0.079.

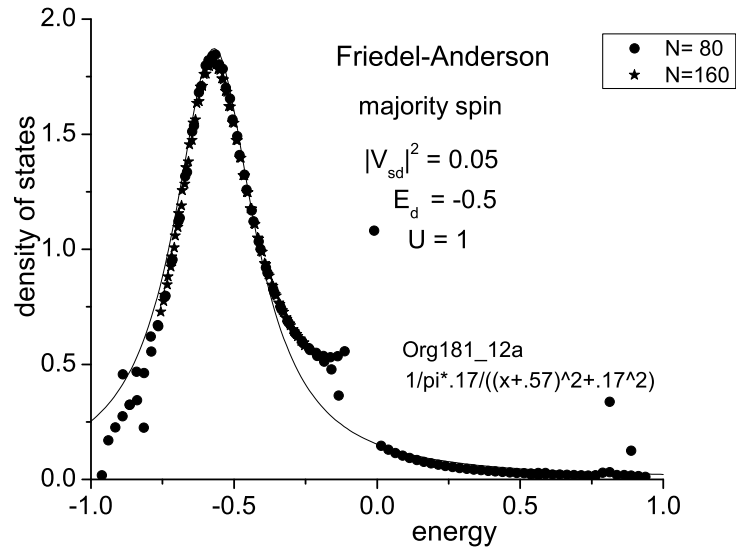


Fig.8a: The density of states for the majority spins for  $|V_{sd}^0|^2 = 0.05$

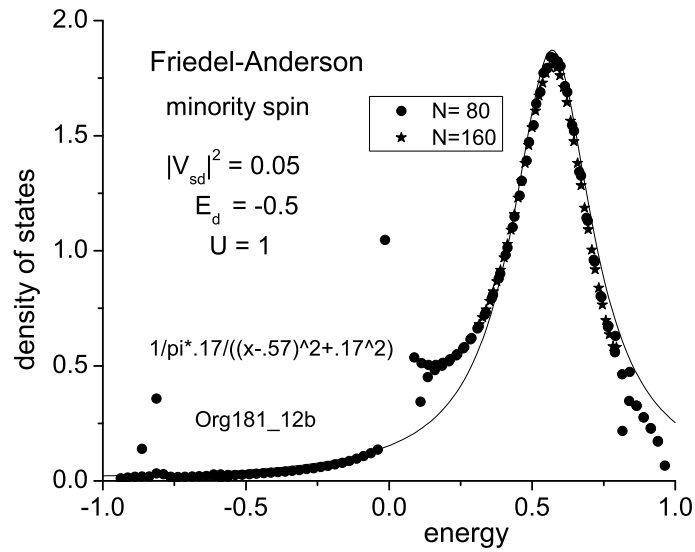


Fig.8b: The density of states for the minority spins for  $|V_{sd}^0|^2 = 0.05$

## 5 Discussion

In the mean field approximation the magnetic state has two d-resonances at the energies  $E_{d,\sigma} = E_d + U n_{d,-\sigma}$ . Since in the symmetric case one has  $n_{d,\sigma} = (1 \mp \mu)/2$  one finds  $E_{d,\sigma} = E_d + U (1 \mp \mu)/2 = \mp U\mu/2 = \pm \mu E_d$  since  $E_d + U/2 = 0$ . So generally the resonances are closer to Fermi energy than  $\pm E_d$ . In our case for the parameters  $E_d = -0.5$ ,  $U = 1$  and  $|V_{sd}^0|^2 = 0.025$  the magnetic moment is within 1%  $\mu \approx 1$  (in units of  $\mu_B$ ) and one expects the resonance almost at  $\pm 0.5$ . The resonance width in mean field is given by  $\Gamma_{mf} = \pi |V_{sd}^0|^2 g(\varepsilon_F)$  where  $g(\varepsilon_F)$  is the density of states of the s-electrons at the Fermi level. This yields for the above parameters  $\Gamma_{mf} = \pi * 0.025 * .5 = 0.039$ . (The matrix element  $V_{sd}^0$  and the density of states are normalized to the atomic volume as the sample volume). This is the same width that one expects for a Friedel resonance with  $|V_{sd}^0|^2 = 0.025$ . Indeed in Fig.7 the Friedel resonance has a  $\Gamma$ -value of  $\Gamma_F = 0.044$ . This agrees within 10% or 0.005 with the numerical result.

The important result is that the resonance width of the minority and majority spins is larger than the Friedel resonance width by a factor of two. Therefore the obtained resonance width is also twice the mean field resonance width. This suggests that the any calculation which uses mean field yields an incorrect density of states. It will be interesting to check how the spin-density functional theory is affected by this result because the latter uses the mean field approximation.

Since the Coulomb interaction broadens the d-resonance by a factor of two it also reduces the height of the resonance by the same factor of two. Therefore it is very plausible that the mean field theory overestimates the tendency to form a magnetic moment. If the criterion for the formation of a magnetic moment,  $UN_d > 1$ , is accepted then one expects that the critical Coulomb energy for the formation of a magnetic moment is increased by a factor of two. This was the previous result by the author [21].

In the density of states of the majority and minority spins in Fig.6ab and Fig.8a,b one observes a scattering and a small maximum at zero energy. This is probably due to the fact that I used a constant cell width for the Wilson states. This means that I average over all states within an energy cell of the width  $\delta E = 2/N$ . This is definitely a poor approximation for the two energy cells  $\mathfrak{E}_{N/2-1}$  and  $\mathfrak{E}_{N/2}$  (which touch the Fermi level). Wilson avoids this problem by using a logarithmic energy scale. However, the present method to evaluate the density of states does not work for an energy-dependent cell width. Details of this question will have to be clarified in the future.

## 6 Conclusion

In this paper the density of states of the Friedel-Anderson impurity is calculated in the magnetic ground state. The magnetic ground state is enforced by the application of a magnetic field whose Zeeman energy is an order of magnitude larger than the Kondo energy. (For the parameters chosen in the numerical calculation the effect of the magnetic field is so small that it can be neglected). The FAIR ground state is the eigenstate of a Hamiltonian

$H'_0$ . To construct this Hamiltonian two artificial Friedel resonance states  $a_{0,\uparrow}^\dagger$  and  $b_{0,\downarrow}^\dagger$  are reverse engineered out of the original spin-up and spin-down conduction bands. There is a numerical procedure to optimize these two FAIR states. When this is done one has an extremely simple Hamiltonian  $H'_0$ . In  $H'_0$  only the two s-states  $a_{0,\uparrow}^\dagger$  and  $b_{0,\downarrow}^\dagger$  interact with the d-state. These states  $a_{0,\uparrow}^\dagger$ ,  $b_{0,\downarrow}^\dagger$ ,  $d_\uparrow^\dagger$  and  $d_\downarrow^\dagger$  are called the nest states.  $H'_0$  is diagonal in the (modified) conduction band electrons  $\{a_{j,\uparrow}^\dagger\}$  and  $\{b_{j,\downarrow}^\dagger\}$ .

A perturbation Hamiltonian  $H'_1 = H_{FA} - H'_0$  which is the difference between the original FA-Hamiltonian and  $H'_0$ , has zero energy expectation value in the FAIR ground state. In addition it is shown in second order self-consistent perturbation theory (see appendix C) that the total occupation of all perturbation states is only of the order of  $10^{-4}$ , i.e. the FAIR ground state has still an amplitude of 0.9998. This is important when an electron or hole is injected into the ground state.

The excitation spectrum is obtained by injecting an electron or a hole into the ground state. The resulting excited states interact via the perturbation Hamiltonian  $H'_1$  and yield a spectrum of energy resonances. It turns out that the injection of an electron into the spin-up conduction band creates also transition between the spin-down conduction band and the nest states.

The resulting density of states possesses the shape of a resonance curve. However, the resonance width is about twice the value of the mean-field theory. As a consequence the height of the resonance density of states is reduced by a factor of two. Since the formation of a magnetic moment depends on the product of the Coulomb interaction and the density of d-states, one would expect that the mean field overestimates the tendency towards a magnetic moment. Indeed I observed in the first paper about the magnetic ground state that the formation of a magnetic moment requires about twice the Coulomb energy that the mean field theory predicts. This consorts well with the present finding of the reduced resonance density of states.

The next step in the future investigation is the calculation of the density of states of the Kondo resonance within the FAIR model. For this calculation one has to use a Wilson spectrum with a logarithmic energy scale.

# A The FAIR approach

## A.1 The Friedel impurity

The basic idea of the FAIR method can be best explained for a Friedel resonance with the Hamiltonian

$$H_F = \sum_{\nu=0}^{N-1} \varepsilon_\nu c_\nu^\dagger c_\nu + E_d d^\dagger d + \sum_{\nu=0}^{N-1} V_\nu^{sd} [d^\dagger c_\nu + c_\nu^\dagger d]$$

This is done in the following steps:

1. from the free (or s-) electron basis an artificial Friedel resonance (**FAIR**) state is constructed with  $a_0^\dagger = \sum_\nu \alpha_0^\nu c_\nu^\dagger$  together with a full orthonormal basis  $\{a_i^\dagger\}$  so that the free electron-electron Hamiltonian  $H_{fe} = \sum_{\nu=0}^{N-1} \varepsilon_\nu c_\nu^\dagger c_\nu$  takes the form

$$H_{fe} = \sum_{i=1}^{N-1} E_i^{(a)} a_i^\dagger a_i + E_0^{(a)} a_0^\dagger a_0 + \sum_{i=1}^{N-1} V_i^{(a)fr} [a_0^\dagger a_i + a_i^\dagger a_0]$$

The requirement that the matrix elements between different  $a_j^\dagger$  and  $a_k^\dagger$  ( $i, k \neq 0$ ) vanish has the consequence that a given FAIR state  $a_0^\dagger$  determines uniquely the full basis  $\{a_i^\dagger\}$ . In the new basis the total Friedel Hamiltonian takes the form

$$H_F = H'_0 + H'_1$$

where

$$H'_0 = \sum_{i=1}^{N-1} E_i^{(a)} a_i^\dagger a_i + E_0^{(a)} a_0^\dagger a_0 + E_d d^\dagger d + V_0^{(a)sd} [d^\dagger a_0 + a_0^\dagger d] \quad (9)$$

The perturbation Hamiltonian has the form

$$H'_1 = \left\{ \sum_{i=1}^{N-1} V_i^{(a)fr} [a_0^\dagger a_i + a_i^\dagger a_0] + \sum_{i=1}^{N-1} V_i^{(a)sd} [d^\dagger a_i + a_i^\dagger d] \right\} \quad (10)$$

Here the new matrix elements are given as  $V_i^{(a)fr}$  and  $V_i^{(a)sd}$ .

2. A trial state  $\Psi_F$  is defined as

$$\Psi_F = [A_0 a_0^\dagger + A_d d^\dagger] |\mathbf{0}_a\rangle \quad (11)$$

where  $|\mathbf{0}_a\rangle = \prod_{j=1}^{n-1} a_j^\dagger |\Phi_0\rangle$ ,  $n = N/2$ . The right side is abbreviated as

$$\Psi_F = \sum_{\alpha=0,d} A_{\alpha,\beta} \Psi_\alpha$$

where, for example, for  $\alpha = d$  one has  $\Psi_d = d^\dagger |\mathbf{0}_a\rangle$

3. The energy expectation value  $E_{00} = \langle \Psi_F | H_F | \Psi_F \rangle$  of the  $H'_0$  with respect to the trial state  $\Psi_F$  is calculated. The contribution of  $H'_1$  is not included. This results in a  $2 \times 2$  secular matrix

$$\begin{pmatrix} \sum_{i=1}^{n-1} E_i + E_0^{(a)} & V_0^{(a)sd} \\ V_0^{(a)sd} & \sum_{i=1}^{n-1} E_i + E_d \end{pmatrix}$$

whose lowest eigenvalue yields  $E_{00}$  and the corresponding eigenvector yields the coefficients  $A_0, A_d$ .

4. The FAIR state is rotated (by variation) in the  $N$ -dimensional Hilbert space until the lowest eigenvalue of the secular matrix reaches a minimum.

It has been shown by the author [24], [25] that this procedure results in the **exact**  $n$ -particle ground state of a Friedel Hamiltonian (given by (11)). The matrix elements of the perturbation Hamiltonian  $H'_1$  between this ground state and any excited state vanish.

It is interesting to look at the result in some more detail.

- The states  $a_i^\dagger$  ( $i \neq 0$ ) enter the secular matrix only through the total energy of the occupied states  $\sum_{i=1}^{n-1} E_i$  and contribute only the the background energy.
- The coefficients and the relative weight of the states  $a_0^\dagger$  and  $d^\dagger$  are only determined by the energies of the FAIR and the d-state  $E_0^{(a)}, E_d$  and their coupling  $V_0^{(a)sd}$ .

In a way one can say that the states  $a_i^\dagger$  prepare just the background - a kind of nest - for  $a_0^\dagger$  and  $d^\dagger$ . The secular matrix represents an effective Hamiltonian for these two states in the nest. In the following I will call the secular matrix without the kinetic energy  $\sum_{i=1}^{n-1} E_i$  the **nest Hamiltonian**.

$$H^{nst} = \begin{pmatrix} E_0^{(a)} & V_0^{(a)sd} \\ V_0^{(a)sd} & E_d \end{pmatrix}$$

The state  $a_0^\dagger$  represents an artificially inserted Friedel resonance state. Therefore I call  $a_0^\dagger$  a "**F**riedel **A**rtificially **I**nserted **R**esonance" state or **FAIR**-state. The use of the FAIR-states is at the heart of my approach to the FA- and Kondo impurity problem. Therefore I call this approach the **FAIR** method.

## A.2 From mean field to the FAIR magnetic state

The Hamiltonian of the Friedel-Anderson impurity is given in equ. (1). One obtains the mean-field Hamiltonian from equ.(??) by replacing  $n_{d\uparrow} n_{d\downarrow} \Rightarrow n_{d\uparrow} \langle n_{d\downarrow} \rangle + \langle n_{d\uparrow} \rangle n_{d\downarrow} - \langle n_{d\uparrow} \rangle \langle n_{d\downarrow} \rangle$ . After adjusting  $\langle n_{d\uparrow} \rangle$  and  $\langle n_{d\downarrow} \rangle$  self-consistently one obtains two Friedel resonance Hamiltonians with a spin-dependent energy of the  $d_\sigma$ -state:  $E_{d,\sigma} = E_d + U \langle n_{d,-\sigma} \rangle$ .

$$H_{mf} = \sum_\sigma \left\{ \sum_{\nu=1}^N \varepsilon_\nu c_{\nu\sigma}^\dagger c_{\nu\sigma} + E_{d\sigma} d_\sigma^\dagger d_\sigma + \sum_{\nu=1}^N V_{sd}(\nu) [d_\sigma^\dagger c_{\nu\sigma} + c_{\nu\sigma}^\dagger d_\sigma] \right\}$$

The mean-field wave function is a product of two Friedel ground states for spin up and down  $\Psi_{mf} = \Psi_{F\uparrow} \Psi_{F\downarrow}$ .

Now we express each Friedel ground state  $\Psi_{F\sigma}$  by the FAIR solution, for example

$$\Psi_{F,\uparrow} = \left( A_{a,\uparrow} a_{0,\uparrow}^\dagger + A_{d,\uparrow} d_\uparrow^\dagger \right) \prod_{i=1}^{n-1} a_{i,\uparrow}^\dagger \Phi_0$$

For the two Friedel states in the mean-field wave function I use the form of equ. (11) and obtain for the mean-field solution

$$\begin{aligned} \Psi_{mf} &= \left[ \left( A_{a,\uparrow} a_{0,\uparrow}^\dagger + A_{d,\uparrow} d_\uparrow^\dagger \right) \prod_{i=1}^{n-1} a_{i,\uparrow}^\dagger \right] \left[ \left( A_{b,\downarrow} a_{0,\downarrow}^\dagger + A_{s,\downarrow} d_\downarrow^\dagger \right) \prod_{i=1}^{n-1} b_{i,\downarrow}^\dagger \right] \Phi_0 \\ &= \left[ A_{a,b} a_{0\uparrow}^\dagger b_{0\downarrow}^\dagger + A_{a,d} a_{0\uparrow}^\dagger d_\downarrow^\dagger + A_{d,b} d_\uparrow^\dagger b_{0\downarrow}^\dagger + A_{d,d} d_\uparrow^\dagger d_\downarrow^\dagger \right] |\mathbf{0}_{a,\uparrow} \mathbf{0}_{b,\downarrow}\rangle \end{aligned} \quad (12)$$

where  $\{a_{i,\uparrow}^\dagger\}$  and  $\{b_{i,\downarrow}^\dagger\}$  are two (different) bases of the  $N$ -dimensional Hilbert space. This solution can be rewritten as equation (4).

In the mean-field solution  $\Psi_{mf}$  the coefficients  $A_{\alpha,\beta}$  are restricted by two conditions  $A_{a,\uparrow}^2 + A_{d,\uparrow}^2 = 1$  ( $A_{b,\downarrow}^2 + A_{d,\downarrow}^2 = 1$ ). Therefore this state does not describe well the correlation effects.

In contrast the state (4) opens a wide playing field for improving the solution: (i) The FAIR states  $a_0^\dagger$  and  $b_0^\dagger$  can be individually optimized, each one defining a whole basis  $\{a_i^\dagger\}$  and  $\{b_j^\dagger\}$ . This yields a much better treatment of the correlation effects. The resulting state is denoted as the (potentially) magnetic state  $\Psi_{MS}$ . The magnetic state  $\Psi_{MS}$  has the same structure as the mean field solution  $\Psi_{mf}$ ; the only difference is that its components are optimized for the Friedel-Anderson Hamiltonian.

## B Self-consistent Perturbation

In the construction of the magnetic ground state  $\Psi_{MS}$  only the Hamiltonian  $H'_0$  (equ. 2) has been used. The expectation value of the "perturbation" Hamiltonian  $H'_1$  is zero,  $\langle \Psi_{MS} | H'_1 | \Psi_{MS} \rangle = 0$  where  $H'_1 = H_{1\uparrow} + H_{1\downarrow}$  and

$$H'_{1,\sigma} = \sum_{j=1}^{N-1} V_j^{(a)fr} \left[ a_{0,\sigma}^\dagger a_{j,\sigma} + a_{j,\sigma}^\dagger a_{0,\sigma} \right] + \sum_{j=1}^{N-1} V_j^{(a)sd} \left[ d_\sigma^\dagger a_{j,\sigma} + a_{j,\sigma}^\dagger d_\sigma \right] \quad (13)$$

But  $H'_1$  yields transitions from the ground state  $\Psi_{MS}$  into excited states. From equ. (13) one recognizes that  $H'_{1\uparrow}$  only permits transitions between the nest  $(d_\uparrow^\dagger, a_{0\uparrow}^\dagger)$  and a band state  $a_{j\uparrow}^\dagger$  but no transition among band states.

If one considers only final states through this transitions which are linear in  $H'_1$  then Fig.9 shows the possible final states. For the spin-up band this are the transitions from the

nest state into an electron excitation  $a_j^\dagger$ , leaving the spin-up part of the nest empty or a transition from an occupied state by creating a hole  $a_j$  and filling both state  $a_{0\uparrow}^\dagger$  and  $d_\uparrow^\dagger$  of the spin-up part of the nest. The corresponding states are generated for the spin-down band.

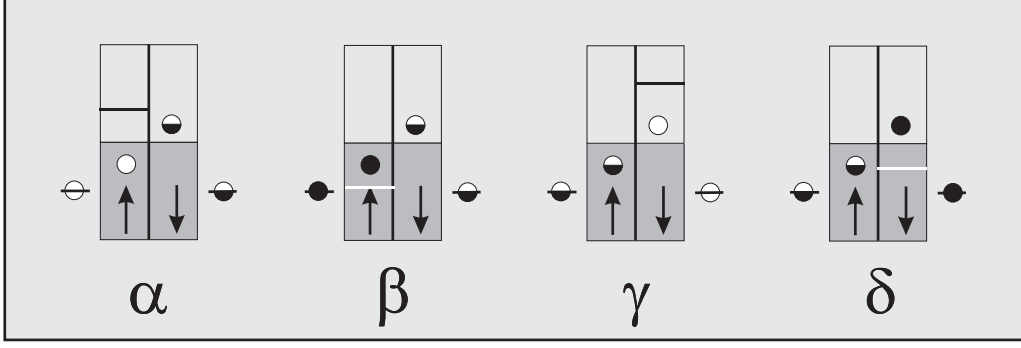


Fig.9: Final states which can be obtained by transitions from the ground state  $\Psi_{MS}$  through the perturbation Hamiltonian  $H'_1$ .

As an example we consider the transitions in the spin-up band. Applying  $H'_{1\uparrow}$  to the ground state  $\Psi_{MS}$  yields

$$H'_{1\uparrow}\Psi_{MS} = \sum_{j=1}^{N-1} \left\{ \begin{aligned} & \left[ V_j^{(a)fr} A_{a,b} + V_j^{(a)sd} A_{d,b} \right] a_{j,\sigma}^\dagger b_{0\downarrow}^\dagger \\ & + \left[ V_j^{(a)fr} A_{a,d} + V_j^{(a)sd} A_{d,d} \right] a_{j,\sigma}^\dagger d_\downarrow^\dagger \\ & + \left( -V_j^{(a)fr} A_{d,b} + V_j^{(a)sd} A_{a,b} \right) a_{j,\uparrow} a_{0\uparrow}^\dagger d_\uparrow^\dagger b_{0\downarrow}^\dagger \\ & + \left( -V_j^{(a)fr} A_{d,d} + V_j^{(a)sd} A_{a,d} \right) a_{j,\uparrow} a_{0\uparrow}^\dagger d_\uparrow^\dagger d_\downarrow^\dagger \end{aligned} \right\} |0_{a,\uparrow} 0_{b,\downarrow}\rangle$$

The top two lines represent an electron excitation, shown as the left state in Fig.9 and the bottom two lines a hole excitation shown as the second state in Fig.9. The final states and the corresponding matrix elements are collected in table III.

$\Psi_i$	$\Psi_f$	$\langle \Psi_i   H'_1   \Psi_f \rangle$	excitation
$\Psi_{MS}$	$a_{j\uparrow}^\dagger b_{0\downarrow}^\dagger  0_{a,\uparrow} 0_{b,\downarrow}\rangle$	$\left( V_j^{(a)fr} A_{a,b} + V_j^{(a)sd} A_{d,b} \right)$	electron, $j \geq n$
$\Psi_{MS}$	$a_{j,\uparrow}^\dagger d_\downarrow^\dagger  0_{a,\uparrow} 0_{b,\downarrow}\rangle$	$\left( V_j^{(a)fr} A_{a,d} + V_j^{(a)sd} A_{d,d} \right)$	electron, $j \geq n$
$\Psi_{MS}$	$a_{j,\uparrow} a_{0\uparrow}^\dagger d_\uparrow^\dagger b_{0\downarrow}^\dagger  0_{a,\uparrow} 0_{b,\downarrow}\rangle$	$\left( -V_j^{(a)fr} A_{d,b} + V_j^{(a)sd} A_{a,b} \right)$	hole, $0 < j < n$
$\Psi_{MS}$	$a_{j,\uparrow} a_{0\uparrow}^\dagger d_\uparrow^\dagger d_\downarrow^\dagger  0_{a,\uparrow} 0_{b,\downarrow}\rangle$	$\left( -V_j^{(a)fr} A_{d,d} + V_j^{(a)sd} A_{a,d} \right)$	hole, $0 < j < n$

Table III: For the spin-up band the final states  $\Psi_f$ , and the matrix elements of  $H'_1$  between the ground state  $\Psi_{MS}$  and the final states  $\Psi_f$  are listed.

The final states still have to be expanded into new eigenstates of the nest plus band. For the spin-down band one obtains equivalent transitions.

There are two important aspects of this result, (i) there are always two transitions into each final state, for example  $a_{0\uparrow}^\dagger \rightarrow a_{j\uparrow}^\dagger$  and  $d_\uparrow^\dagger \rightarrow a_{j\uparrow}^\dagger$ . These two transitions interfere and cancel each other almost completely (as will be shown below). (ii) The first two final states in table III (as well as the third and fourth final state) are not eigenstates of  $H'_0$ . One has to expand these final states in terms of the eigenstates of the nest, for example

$$\begin{array}{|c|} \hline a_{j,\uparrow} a_{0\uparrow}^\dagger d_\uparrow^\dagger b_{0\downarrow}^\dagger |\mathbf{0}_{a,\uparrow} \mathbf{0}_{b,\downarrow}\rangle \\ \hline a_{j,\uparrow} a_{0\uparrow}^\dagger d_\uparrow^\dagger d_\downarrow^\dagger |\mathbf{0}_{a,\uparrow} \mathbf{0}_{b,\downarrow}\rangle \\ \hline \end{array} \iff \begin{array}{l} a_{j,\uparrow} \Psi_{2/1}^{(1)} \\ a_{j,\uparrow} \Psi_{2/1}^{(2)} \end{array}$$

This is in complete analogy to the calculation of the excitations in section III.

In Fig.10 the logarithm of the effective matrix element is plotted for the first transition in table III. This represents an electron excitation which is restricted to positive energies. As one recognizes the effective matrix elements are strongly reduced in the energy range in which transitions are possible. The value of  $V_{eff}$  lies in the range between  $10^{-3}$  and  $10^{-4}$  while the original matrix elements for  $V_{sd}$  are 0.025. This applies for all eight possible excitations. In the energy range where an excitation is permitted the matrix elements are strongly reduced. Among the eight possible transitions there is only one transition whose matrix elements exceed  $10^{-3}$ . This is the second one in table III where the matrix element reaches values of  $2 \times 10^{-3}$ , still much smaller than the original matrix elements.

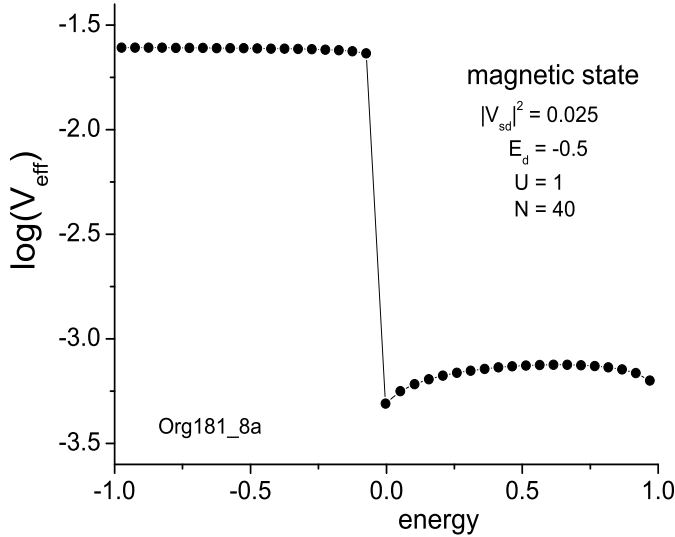


Fig.10: The logarithm of the effective matrix elements for a transition from the ground state  $\Psi_{MS}$  into the excited state  $a_{j\uparrow}^\dagger b_{0\downarrow}^\dagger |\mathbf{0}_{a,\uparrow} \mathbf{0}_{b,\downarrow}\rangle$ . This transition is only possible for positive energies, and there the interference between the the d-state  $d_\uparrow^\dagger$  and the FAIR state  $a_{0\uparrow}^\dagger$  cancels the transition almost completely.



The strong reduction of the matrix elements is due to the introduction of the FAIR states which compensate the transitions involving the d-states. It is also the reason why the magnetic ground state is so well represented by  $\Psi_{MS}$ .

With the eigenenergies of the states in Fig.9 and the matrix elements for the transition from the ground state  $\Psi_{MS}$  into these states one can now perform a self-consistent perturbation calculation. The number of excited states is  $2(N-1)$  for each spin-band. One can build the full secular matrix for these states which consists of  $4(N-1)+1$  states, where the additional one is the ground state. The result for our standard example ( $E_d = -0.5$ ,  $U = 1$ ,  $|V_{sd}^0|^2 = 0.025$ ,  $N = 40$ ) is rather dramatic. The weight of all  $4(N-1)$  excitations together is only about  $10^{-4}$ . The amplitude of  $\Psi_{MS}$  after diagonalization is 0.99985. This demonstrates the FAIR solution is an excellent approximation to the ground state.

## C Green's functions

With the secular Hamiltonian  $H^{xct}$  in section 3.1 one can construct the Green's functions (GF) of the excitations  $\varphi_\nu$

$$\sum_\nu (\varepsilon + is - H^{xct})_{\mu,\nu} G_{\nu,\kappa} = \delta_{\mu,\kappa}$$

or

$$\mathbf{G} = (\varepsilon + is - \mathbf{H}^{xct})^{-1}$$

The resulting diagonal elements of  $\mathbf{G}$  are the Green's function of the excitations, for example  $G_{11}(\varepsilon)$  is the Green's function of  $\Psi_{2/1}^{(1)}$ . Since the  $G_{\mu,\mu}(\varepsilon)$  are a function of the energy the above relation is not very practical for a numerical nor analytical calculation of  $G_{\mu,\mu}(\varepsilon)$ . For a numerical evaluation it is much easier to calculate the eigenvalues  $E_\mu^{xct}$  and eigenvectors  $\psi_\mu$  of  $H^{xct}$  where  $\psi_\mu = \sum_\nu \psi_\mu^\nu \varphi_\nu$ . Then the Green's function  $G_{\mu,\mu}$  of the excitation can be expressed as

$$G_{\nu,\nu}(\varepsilon) = \sum_\nu \frac{|\psi_\mu^\nu|^2}{\varepsilon - E_\mu^{xct} + is}$$

Each energy eigenvalue contributes to the spectrum of the state  $\varphi_\nu$ .

For the particle density of states we need the Green's function (or the spectrum) of the  $\frac{N}{2}$  states  $a_{j\uparrow}^\dagger \Psi_{MS}$  and  $a_{0\uparrow}^\dagger \Psi_{MS}$  and  $d_{\uparrow}^\dagger \Psi_{MS}$ . The  $N/2$  electron Green's functions  $G_{a_j, a_j}(\varepsilon)$  follow directly from the above calculation. The  $G_{a_0, a_0}(\varepsilon)$  and  $G_{d, d}(\varepsilon)$  for spin up have to be derived from the Green's functions of  $\Psi_{2/1}^{(1)}$  and  $\Psi_{2/1}^{(2)}$ .

In Fig.3 a spin-up electron is injected into the nest. This electron can be injected into the  $a_{0\uparrow}^\dagger$  or the  $d_{\uparrow}^\dagger$  state. These processes yield complementary amplitudes of

$$\begin{aligned} a_{0\uparrow}^\dagger \Psi_{MS} &= \left( A_{d,b} a_0^\dagger d_{\uparrow}^\dagger b_{0\downarrow}^\dagger + A_{d,d} a_0^\dagger d_{\uparrow}^\dagger d_{\downarrow}^\dagger \right) |\mathbf{0}_{a,\uparrow} \mathbf{0}_{b,\downarrow}\rangle \quad \text{for } a_0^\dagger \\ d_{\uparrow}^\dagger \Psi_{MS} &= - \left( A_{a,b} a_{0\uparrow}^\dagger d_{\uparrow}^\dagger b_{0\downarrow}^\dagger + A_{a,d} a_{0\uparrow}^\dagger d_{\uparrow}^\dagger d_{\downarrow}^\dagger \right) |\mathbf{0}_{a,\uparrow} \mathbf{0}_{b,\downarrow}\rangle \quad \text{for } d_{\uparrow}^\dagger \end{aligned}$$

Each of the two resulting states has to be expanded in the two eigenstates  $\Psi_{2/1}^{(1)}$  and  $\Psi_{2/1}^{(2)}$  of the nest. For example, the amplitudes for  $a_{0\uparrow}^\dagger \Psi_{MS}$  are obtained through the scalar product between  $a_{0\uparrow}^\dagger \Psi_{MS}$  and  $\Psi_{2/1}^{(\alpha)}$ . Then they can make a transition into any of the other states with a single excitation, for example the state  $a_{j\uparrow}^\dagger \Psi_{MS}$ . Again the resulting amplitudes interfere. So the particle components of the GFs  $G_{a_0, a_0}(\varepsilon)$  and  $G_{d, d}(\varepsilon)$  are composed of the GFs of  $\Psi_{2/1}^{(\alpha)}$  with a weight which is the square of the scalar product between the amplitude in equ. (5) and  $\Psi_{2/1}^{(\alpha)}$ . These GFs  $G_{a_0, a_0}(\varepsilon)$  and  $G_{d, d}(\varepsilon)$  have also a hole component.

## References

- [1] J. Friedel, Philos. Mag. 43, 153 (1952); Adv. Phys. 3, 446 (1954); Philos. Mag. Suppl. 7, 446 (1954); Can. J. Phys. 34, 1190 (1956); Nuovo Cimento Suppl. 7, 287 (1958); J. Phys. Radium 19, 573 (1958), The electronic structure of the transition metals and their alloys and of the heavy metals
- [2] P. W. Anderson, Phys. Rev. 124, 41 (1961), Localized Magnetic States in Metals
- [3] J. Kondo, Prog. Theor. Phys. 32, 37 (1964) , Resistance Minimum in dilute magnetic alloys.
- [4] K. Yosida, Phys. Rev. 147, 223 (1966), Bound state due to the s-d exchange interaction
- [5] C. M. Varma and Y. Yafet, Phys. Rev. B13, 2950 (1976), Magnetic susceptibility of mixed rare-earth compounds
- [6] K. Schoenhammer, Phys. Rev. B 13, 4336 (1976) , Variational Ansatz for the Anderson model of chemisorption
- [7] M. D. Daybell, and W. A. Steyert, Rev. Mod. Phys. 40, 380 (1968) , Localized Magnetic Impurity States In Metals: Some Experimental Relationships
- [8] A. J. Heeger, in Solid State Physics, ed. by F. Seitz, D. Turnbull, and H. Ehrenreich (Academic, New York, 1969), Vol 23, p284 , Localized moments and nonmoments in metals: the Kondo effect
- [9] M. B. Maple, in "Magnetism", edited by G. T. Rado and H. Suhl (Academic, New York, 1973), Vol. V, p. 289, Paramagnetic Impurities in Superconductors
- [10] P. W. Anderson, Rev. Mod. Phys. 50, 191 (1978) , Local moments and localized states
- [11] G. Gruener and A. Zavadowski, Prog. Low Temp. Phys. 7B, 591 (1978), Low temperature properties of Kondo alloys

- [12] P. Coleman, J. Magn. Magn. Mat. 47, 323 (1985),
- [13] A. C. Hewson, The Kondo problem to heavy Fermions, Cambridge University Press, 1993,
- [14] S. K. Kwon and B. I. Min, Phys. Rev. Lett. 84, 3970 (2000), Origin of the giant moments of Fe impurities on and in Cs films
- [15] R. B. Sahu and L. Kleinman, Phys. Rev. B67, 094424 (2003), Non-enhancement of magnetic moments on transition metal impurities by alkali metal hosts
- [16] M. E. McHenry, J. M. MacLaren, D. D. VVendensky, M. E. Eberhart and M. L. Prueitt, Phys. Rev. B40, 10111 (1989), Formation of local moments on iron in alkali-metal hosts
- [17] R. Podloucky, R. Zeller and P. H. Dederichs, Phys. Rev. B22, 5777 (1980), Electronic structure of magnetic impurities calculated from first principles
- [18] V. I. Anisimov and P. H. Dederichs, Solid State Commun. , 84, 241 (1992), LDA +U calculations for 4d impurities in Rb
- [19] D. E. Logan, M. P. Eastwood, and M. A. Tusch, J. Phys.: Condens. Matter 10, 2673 (1998) , A local moment approach to the Anderson model
- [20] G. Bergmann, Phys. Rev. B 74, 144420 (2006) , Compact Approximate Solution to the Friedel-Anderson Impuriy Problem
- [21] G. Bergmann, Phys. Rev. B 73, 092418 (2006) , A Critical Analysis of the Mean-Field Approximation for the Calculation of the Magnetic Moment in the Friedel-Anderson Impurity Model
- [22] G. Bergmann and L. Zhang, Phys. Rev. B 76, 064401 (2007) , A Compact Approximate Solution to the Kondo Problem
- [23] K. G. Wilson, Rev. Mod. Phys. 47, 773 (1975), The renormalization group: Critical phenomena and the Kondo problem

- [24] G. Bergmann, Z. Physik B102, 381 (1997), A new many-body solution of the Friedel resonance problem
- [25] G. Bergmann, Eur. Phys. J. B2, 233 (1998), Geometrical derivation of a new ground-state formula fo the n-electron Friedel resonance